IIE Transactions (2004) **36**, 447–455
Copyright © "IIE"
ISSN: 0740-817X print / 1545-8830 online
DOI: 10.1080/07408170490426152

Optimization design of control chart systems

ZHANG WU*, YEE CHEONG LAM, SHENG ZHANG and M. SHAMSUZZAMAN

School of Mechanical and Production Engineering, Nanyang Technological University, Singapore 639798
E-mail: mzwu@ntu.edu.sg

Received November 2001 and accepted November 2003

This article proposes an algorithm to design an integrated control chart system consisting of several individual control charts, each of which is used to monitor a critical process stage in the manufacture of a product. The design algorithm considers all the charts within a system in an integrative and optimal manner. Consequently, the performance characteristics of the system as a whole can be significantly improved and the product quality will be further enhanced. Such an improvement is achieved without requiring additional cost and effort for on-line inspections. Furthermore, the floor operators can utilize and understand the optimal control chart system as easily as they do the existing system. Some useful guidelines have also been highlighted to aid the users to adjust the control limits of the control charts in a system.

1. Introduction

The fabrication of a product usually includes many process stages. The integration of all these stages results in a *manufacturing system*. Specifically, in the manufacture of a mechanical part, each stage corresponds to the machining of a dimension. As an example, several process stages are required to fabricate the dimensions of the part shown in Fig. 1(a). Some of the dimensions are critical to the overall quality of the product and the corresponding process stages have to be monitored using control charts. A *control chart system* is the combination of all the charts that are used to monitor the critical stages of a manufacturing system.

Due to differences in production rates and other factors, some stages (e.g., stages with lower production rates) may have more than one parallel stream (e.g., machine). In some applications, a single Shewhart chart or group chart is used to monitor the outputs from all the streams of a stage. However, in this article, a separate chart will be applied to the output of each individual stream. This scenario helps to detect and diagnose the out-of-control stream (Montgomery, 2001). Usually, the parallel streams in a single stage have the same mean, standard deviation and target (Runger *et al.*, 1996), and therefore, all of them use an identical control chart. In the machining of the part shown in Fig. 1(a), four critical dimensions x_i ($i = 1$, 2, 3 and 4) are formed in four stages. Dimension x_1 is formed by facing surface 1 using surface 0 as the datum. Dimension x_2 is associated with surface 2 which is machined with reference to surface 1. Then, using surface 2 as the datum, surfaces 3 and 4 are drilled and milled, respectively, and dimensions x_3 and x_4 are determined. It is noteworthy that x_2 depends directly on x_1, and both x_3 and x_4 are directly affected by x_2. Four control charts as a system are used to carry out the on-line monitoring of the processes of the four machining stages x_1 to x_4. Furthermore, since two identical machines are used side by side to mill dimension x_4, control chart 4 has two duplicates, each controls one of the two parallel machines. A block diagram of this control chart system is displayed in Fig. 1(b). All non-functional process stages are ignored in the block diagram and are not included in the design of the control chart system. It is assumed that the quality requirements on the non-functional dimensions can be easily met and on-line monitoring is unnecessary.

In this article, a process means one single-stream stage or one stream in a multi-stream stage. The total number, M, of the processes that are monitored by the control chart system is equal to:

$$M = \sum_{i=1}^{s} g_i, \qquad (1)$$

where, s is the number of functional stages and g_i is the number of streams in the ith stage ($g_i \geq 1$). However, since the g_i streams in the ith stage are monitored by identical control charts (with the same sample size, sampling interval and control limits), there are only s different charts in the control chart system. In Fig. 1(b), the production flow enters the system from the left-hand side. It first goes through stages 1, 2 and 3 sequentially; then, branches into two parallel and identical streams in stage 4; and finally reaches the output point on the right-hand side. The production rate in

*Corresponding author

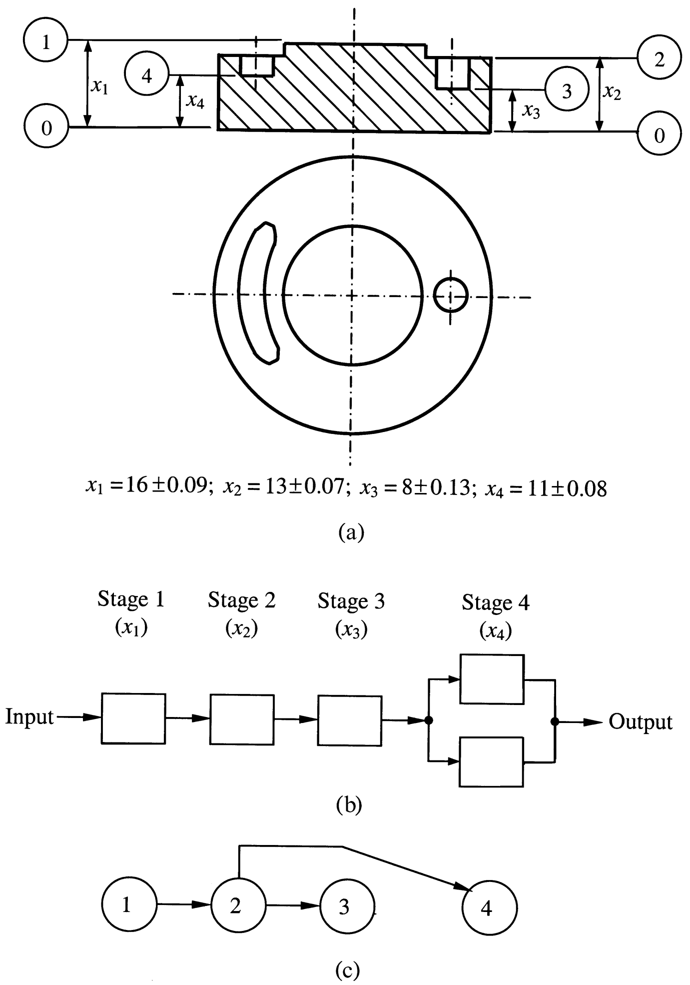

Fig. 1. (a) The dimensions of the part; (b) the process stages; (c) the quality linkages.

each stage may not be exactly the same and buffers may be used between the stages when necessary.

If any process is out of control, the control chart system should produce a signal as quickly as possible, otherwise the overall quality of the product is likely to deteriorate. However, if all the charts in the system report an in-control status, the whole manufacturing system is assumed to be in control and the product quality should be satisfactory.

Conventionally, each individual chart in a system is designed in isolation. For example, the $\bar{X}$ chart is a charting tool for monitoring the process mean shifts and is used most widely in SPC (Statistical Process Control). Its lower control limit *LCL* and upper control limit *UCL* are calculated as follows:

$$LCL = \mu_0 - k\sigma/\sqrt{n}, \quad UCL = \mu_0 + k\sigma/\sqrt{n}, \tag{2}$$

where, n is the sample size, μ_0 and σ are the in-control process mean and standard deviation respectively and k is the control limit coefficient. In conventional chart system designs, k is identical for every individual chart, typically being set at three. However, if all of the charts in a system are designed in an integrated and optimal manner, the overall effectiveness of the system may be improved. The optimization design of the control chart system may result in different k values or allocate a different power to different charts in a system based on the values of certain parameters (e.g., process capability, sampling interval, sample size) that would affect the performance of the control chart system.

The idea of applying multiple univariate control charts to individual variables has been discussed in Montgomery's textbook on SPC (Montgomery, 2001). However, hitherto, little literature can be found in the optimization design of an integrated control chart system for a manufacturing system. Woodall and Ncube (1985) investigated the multivariate CUSUM control procedures and defined the out-of-control condition for a system comprising several charts. Their procedures for independent quality characteristics can be applied to multi-stage manufacturing systems. Nonetheless, in their study, the charting parameters (e.g., control limits) are not designed in an integrative and optimal manner. Instead, identical parameter values are used by individual charts. Hawkins (1991) discussed multivariate quality control based on regression-adjusted variables. The purpose of this technique is to make the controls more effective than those based on individual variables. Nelson (1986), and Mortell and Runger (1995) proposed and developed the group control chart for monitoring the output from multiple streams of a single stage. Runger *et al.* (1996) used principle components analysis to develop control charts that are able to detect both common and special assignable causes in multiple process streams. Zhang (1989), Fong and Lawless (1998), and Lawless *et al.* (1999) discussed the variation transmission through multiple process stages. Wade and Woodall (1993), Ding, Ceglarek and Shi (2002a, 2002b) and Ding, Shi and Ceglarek (2002) have published several papers studying multi-stage processes and the diagnosis problems. Zantek *et al.* (2002) used quality linkages to handle the observed interdependence between the quality characteristics in multi-stage processes. However, these papers did not study the multi-stage processes from the viewpoint of on-line SPC monitoring.

Similar to a single control chart, the power or effectiveness of a control chart system is measured by the average time to signal, *ATS*. In this article, *ATS* is defined as the average time that one of the control charts in the chart system gives an out-of-control signal subsequent to any process in a manufacturing system going out of control (Woodall and Ncube, 1985). When any process is out of control, the users want the control chart system to signal quickly, i.e., to have a small out-of-control *ATS* value. Conversely, when the whole manufacturing system is in control, the users want the chart system to produce minimum false alarms, i.e., to have a large in-control ATS_0 value.

A few assumptions and conventions will be adopted in this article.

1. Since the processes will often operate in the in-control condition for most or relatively long periods of time (Montgomery, 2001), it is assumed that only one process is out of control at any moment in a manufacturing system. It is a conservative assumption, because, if two or more processes are out of control simultaneously (e.g., due to some common mode failures), the out-of-control *ATS* will be even smaller compared with the *ATS* under this assumption.
2. Only the $\bar{X}$ chart will be studied in detail in this study.
3. The underlying probability distribution of the quality characteristic x (e.g., the dimension of a mechanical part) in each process is assumed normal with a constant standard deviation.
4. The g_i parallel streams in the ith stage have the same mean, standard deviation and target and use identical control charts (with same sample size, sampling interval and control limits).

2. Optimization design of the control chart system

In this article, the control chart system is intended to monitor all of the functional processes (or simply, the processes) in a manufacturing system. For the design of this chart system, the following parameters are specified.

- s = number of stages in the control chart system;
- g_i = number of streams in the ith stage;
- h_i = sampling interval of the control chart in the ith stage;
- n_i = sample size of the control chart in the ith stage;
- $\mu_{0,i}$ = in-control process mean in the ith stage;
- σ_i = constant standard deviation of the process in the ith stage;
- d_i = maximum allowable value of the mean shift δ_i in the ith stage;
- p_i = probability of out-of-control occurrence in the ith stage;
- τ = minimum allowable in-control ATS_0;
- $\mathbf{V}_i$ = a vector $[v_1, v_2, \ldots]^T$ indicating the cause stage (upstream influencing stage) numbers. The dimension x_i produced in the ith stage is directly dependent on the dimensions produced in all of these cause stages;
- Δ_i = induced mean shift. It is the mean shift undergone by the ith stage due to (or incurred by) the mean shifts of the cause stages. Δ_i is expressed as a function $f_i(\delta_{v_1}, \delta_{v_2}, \ldots)$ in terms of the output mean shifts of all cause stages.

Most of these specifications can be determined easily. The numbers s and g_i can be found from the block diagram (e.g., Fig. 1(b)). The parameters $h_i, n_i, \mu_{0,i}, \sigma_i$ and τ are those usually required by conventional chart designs. Generally, the sampling interval h_i depends on the rational subgrouping or the production shift. The sample size n_i is decided according to the available resources (e.g., the instrument and manpower) and the expected detection power. The distribution parameters $\mu_{0,i}$ and σ_i are usually estimated from the data observed in pilot runs or the process capability study. The variable τ is specified based on the trade-off between the false alarm rate and detection power. If the cost of handling the false alarms is high, a larger τ should be used in order to reduce the false alarm frequency. However, a large τ may at the same time impair the effectiveness of the control chart. The resultant (or actual) in-control ATS_0 must be equal to or larger than τ. The maximum allowable mean shift d_i indicates the rejectable quality level (the barely tolerated mean shift). It may be determined by the QA (Quality Assurance) engineer directly based on factors such as quality, manufacturing cost and customers' requirements. Or more preferably, d_i is calculated from the specified tolerance and the allowable process capability ratio C_{pk}. Each process must have a minimum allowable value $c_{\text{pk,min}}$ for the process capability ratio. The product quality will degrade significantly if C_{pk} is lower than $c_{\text{pk,min}}$. Usually, $c_{\text{pk,min}}$ is decided by considering, for example, whether the process is an existing one or a new one, or whether the product is critical to safety (Montgomery, 2001). A default value of one may be used for $c_{\text{pk,min}}$. It results in a nonconforming parts per million; *PPM*, value of 2700. For the ith process stage:

$$c_{\text{pk,min},i} = \lfloor USL_i - (\mu_{0,i} + d_i) \rfloor / 3\sigma_i. \tag{3}$$

Here, it is assumed that the in-control process mean $\mu_{0,i}$ coincides with the center between the lower specification limit LSL_i and the upper specification limit USL_i (LSL_i and USL_i can be found in the engineering drawings). Therefore, the maximum allowable mean shift d_i for the ith process stage can be calculated as:

$$d_i = USL_i - \mu_{0,i} - 3\sigma_i c_{\text{pk, min},i} \tag{4}$$

Next, the probability p_i that an out-of-control case takes place in the ith stage is estimated from historical data on out-of-control cases. For example, if in a manufacturing system, 10 out of 25 out-of-control cases occurred in the first stage, then $p_1 \approx 10/25 = 0.4$. If such historical data are not available, it may be reasonable to estimate p_i by the following formula:

$$p_i = g_i / \sum_{j=1}^{s} (g_j). \tag{5}$$

This means that the estimated probability that the out-of-control case happens in the ith stage is proportional to the number of parallel streams in this stage. Finally, the vectors $\mathbf{V}_i$ and the formulae for Δ_i can be determined with the help of the quality linkages (Zantek *et al.*, 2002). For example, the cascade quality linkages in Fig. 1(c) indicate that x_2 is directly affected by x_1, and both x_3 and x_4 are directly affected by x_2. Correspondingly:

$$\mathbf{V}_2 = [1]^T, \quad \mathbf{V}_3 = [2]^T, \quad \mathbf{V}_4 = [2]^T. \tag{6}$$

The formulae for Δ_i can take many forms and may be determined by many different methods. For part machining, these formulae may be determined based on the information of design dimensioning and process planning. For the example in Fig. 1(a):

$$\Delta_2 = f_2(\delta_1) = \delta_1, \quad \Delta_3 = f_3(\delta_2) = \delta_2, \quad \Delta_4 = f_4(\delta_2) = \delta_2. \tag{7}$$

Here, for example, ($\Delta_2 = \delta_1$) indicates that stage 2 will have an induced mean shift of Δ_2 if stage 1 has an output mean shift of δ_1, and Δ_2 is equal to δ_1.

Based on the above specifications, the optimization design of the control chart system can be conducted by using the following nonlinear optimization model:

$$\text{Objective function:} \quad ATS = \text{minimum}, \tag{8}$$

$$\text{Constraint function:} \quad ATS_0 \geq \tau, \tag{9}$$

$$\text{Design variables:} \quad k_1, k_2, \ldots, k_s,$$

where, ATS is the average time to signal of the control chart system when any process in the manufacturing system is out of control (or more specifically, when any process mean μ_i has shifted by an amount of d_i). ATS_0 is the average time to signal when the whole system is in control (or all process means remain in $\mu_{0,i}$).

In the actual optimization search, the design variables $k_1, k_2, \ldots, k_s$ (control limit coefficients) are replaced by the corresponding type-I error probabilities $\alpha_1, \alpha_2, \ldots, \alpha_s$ associated with the s control charts. The variable α_i is the probability that the ith control chart produces an out-of-control signal when the ith process is in fact in control:

$$k_i = \Phi^{-1}(1 - 0.5\alpha_i), \tag{10}$$

where $\Phi^{-1}()$ is the inverse function of the cumulative probability function of the standard normal distribution. Optimizing α_i is equivalent to optimizing k_i, but the former is easier to handle during the optimization search. Because α_i has a finite lower bound (zero) and upper bound (one) for the search (conversely, the upper bound of k_i is infinite) and a simple equation among α_1, α_2, ..., α_s (Equation (12)) can be established easily. The objective of the optimization model is to identify the optimal values for (α_1, α_2, ..., α_s) that will jointly minimize ATS (maximize effectiveness) and ensure ATS_0 (the false alarm rate) so that it is equal to the specification. The underlying idea of the optimization design is to enhance the power of those charts which take a very long period to produce a signal when the corresponding processes become out of control. This procedure must sacrifice the power of some other charts in the system. However, if the α_i values of all charts are adjusted in an integrated and optimal manner, the overall (average) effectiveness of the control chart system will be improved.

The final outputs of the optimization design are the optimal control limits for each control chart. They can be derived from the optimal value of α_i through k_i (see Equation (10)).

$$LCL_i = \mu_{0,i} - k_i\sigma_i/\sqrt{n_i}, \quad UCL_i = \mu_{0,i} + k_i\sigma_i/\sqrt{n_i}. \tag{11}$$

The major step in the optimization procedure is to express the objective function ATS (Equation (8)) and the constraint function ATS_0 (Equation (9)) in terms of $\alpha_1, \alpha_2, \ldots, \alpha_s$. The detailed formulae are derived in the Appendices (Equation (A2) for calculating ATS_0, and Equation (A12) for calculating ATS).

The optimization design can be carried out by using any software for nonlinear constrained programming. In our implementation, a dynamic search algorithm is employed. In this algorithm, the optimal values of α_i of the first $(s-1)$ control charts are searched step by step in $(s-1)$ levels, using the same step size $d\alpha$. The last α_s is finally determined so that the resultant ATS_0 is exactly equal to the specified τ (Equation (9)).

Combining Equations (A1) and (A2) in the Appendix, and replacing ATS_0 by τ, the value of any individual α_i can be expressed in terms of other α_j ($j = 1, 2, \ldots, s, j \neq i$) and τ:

$$\alpha_i = h_i\left[1 - \left(\frac{1 - 1/\tau}{\prod_{j=1,j\neq i}^{s}(1 - \alpha_j/h_j)^{g_j}}\right)^{1/g_i}\right]. \tag{12}$$

This equation can be used to determine the range of possible α_i value in the ith level search. As a simple example, let us consider a manufacturing system with three stages ($s = 3$), where $g_1 = g_2 = g_3 = 1$, $h_1 = 100$, $h_2 = 120$, $h_3 = 200$. There are two levels of searches. The first level is to search the optimal α_1. The maximum possible value of α_1 can be found from Equation (12) by setting both α_2 and α_3 equal to zero (i.e., all the power is allocated to the first chart):

$$\alpha_{1,\max} = 100/\tau. \tag{13}$$

Therefore, α_1 will be searched in the range of [0, $100/\tau$] in the first level. The second level is to search the optimal α_2, while α_1 is given. The maximum possible value $\alpha_{2,\max}$ of α_2 should be determined dynamically, because it is dependent on the current value of α_1 given in the first level. The maximum value $\alpha_{2,\max}$ is also found from Equation (12) by setting α_3 equal to zero:

$$\alpha_{2,\max} = 120(1 - (1 - 1/\tau)/(1 - \alpha_1/100)). \tag{14}$$

Therefore, α_2 will be searched between zero and $\alpha_{2,\max}$ in the second level. Finally, α_3 is directly determined using Equation (12) without any search. That is, α_3 (or α_s in a general case) will take the maximum possible value in order to make full use of the power of the control chart system (determined by the specified τ). In this example:

$$\alpha_3 = 200(1 - (1 - 1/\tau)/[(1 - \alpha_1/100)(1 - \alpha_2/120)]). \tag{15}$$

It is clear that the resultant design point (α_1, α_2, α_3) will ensure that ATS_0 is equal to τ.

The overall optimization search is outlined as follows:

Step 1. Specify s, g_i, h_i, n_i, $\mu_{0,i}$, σ_i, d_i, p_i, τ, $\mathbf{V}_i$ and Δ_i.

Step 2. Initialize $ATS_{\min}$ as a large number, say 1000 000. $ATS_{\min}$ is used to record the minimum ATS.

Step 3. Carry out the searches in $(s-1)$ levels.

3.1 Each design point $(\alpha_1, \alpha_2, \ldots, \alpha_s)$ will automatically make ATS_0 equal to τ.

3.2 Calculate ATS by Equation (A12) in the Appendix.

3.3 If this ATS value is smaller than the current $ATS_{\min}$, replace $ATS_{\min}$ by ATS and record the current design point $(\alpha_1, \alpha_2, \ldots, \alpha_s)$ as the temporary optimal solution.

Step 4. When the whole search is completed, the optimal design point $(\alpha_1, \alpha_2, \ldots, \alpha_s)$ is finalized.

Step 5. Calculate the control limits of the s control charts using Equations (10) and (11).

This search algorithm is simple and reliable. A computer program *system.c* written in the C language has been developed to carry out the optimization design. The value of the step size $d\alpha$ is decided so that the total number of search points is always limited to 100 000 regardless of the number of α_i. Usually, an optimal solution is obtained in a few CPU seconds using a personal computer. The program *system.c* is available by contacting the authors.

3. Sensitivity study

This section will study the effects of six parameters (g_i, h_i, n_i, σ_i, d_i and p_i) on the performance of the control chart system. Each of these parameters has a low value, a nominal value and a high value, as shown in Table 1.

The nominal value denotes the value under normal circumstances. The nominal value of g_i is equal to its low value, because it is assumed that there is usually only one stream in a stage, unless the production rate in this stage is much lower than that in other stages.

ATS_0 can be calculated from the in-control average run length, ARL_0, that is the average number of samples counted from the beginning of the process to the first false alarm:

$$ATS_0 = h \times ARL_0. \tag{16}$$

In the sensitivity study, if the sampling interval h_i takes its nominal value of 175 time units (the time unit is determined by the applications) and ARL_0 assumes a typical value of 370 as in a 3σ $\bar{X}$ chart, ATS_0 is found to be 64 750 by Equation (16). Therefore, the value of τ (the minimum allowable in-control average time to signal) is fixed at 64 750 throughout the sensitivity study.

Table 1. The parameter values

Parameter	*Low*	*Nominal*	*High*
g_i	1	1	4
h_i	50	175	300
n_i	3	6	10
σ_i	0.01	0.025	0.04
d_i	0.01	0.03	0.05
p_i	0.1	0.5	0.9

The performance of a two-stage manufacturing system will be studied for six different cases. The two stages are assumed to be independent of each other in the sensitivity study. In each case, all the parameters take their nominal values in both stages, except that one selected parameter (called the *active parameter*) takes its low value in stage 1 and high value in stage 2. For example, in case 1, the first parameter g_i is designated as the active parameter. Therefore,

$$\begin{aligned} g_1 &= 1, \quad g_2 = 4; \\ h_1 &= h_2 = 175; \\ n_1 &= n_2 = 6; \\ \sigma_1 &= \sigma_2 = 0.025; \\ d_1 &= d_2 = 0.03; \\ p_1 &= p_2 = 0.5. \end{aligned} \tag{17}$$

Each case will be investigated for two different control chart systems. The first one is the conventional system, where the α_i values (or equivalently, the control limit coefficients) for the two control charts are made equal. The second one is the optimal system, in which the α_i values of the two control charts are determined by the optimization design proposed in this article. Both control chart systems make ATS_0 equal to $\tau(= 64\,750)$. The ratio R between the out-of-control ATS values resulting from each control chart system would be calculated as:

$$R = ATS_{\text{optimal}}/ATS_{\text{convention}}. \tag{18}$$

Obviously, if R is less than one, the optimal control chart system will outperform the conventional system when the corresponding active parameter has different values in different stages in a manufacturing system. The R values for all six cases are listed in Table 2 under column (7). It can be observed that in all of the six cases, the optimal control chart system achieves an obvious improvement in the effectiveness compared to the conventional system. It is especially the case if any of the four parameters h_i, n_i, σ_i or d_i has different values in the two stages, the optimal control chart system will have a substantially smaller ATS than the conventional system. Among all the parameters, d_i (the maximum allowable mean shift) promises the greatest potential for using the optimal control chart system. A reduction of ATS by 33.1% can be achieved, when d_i has different values ($d_1 = 0.01$, $d_2 = 0.05$ in case 5) and all other parameters are fixed. The performance of the optimal control chart system is relatively less sensitive to the parameters g_i and p_i. The actual R value would differ for different systems and circumstances. However, it is believed that the optimal control chart system would be effective in general and beneficial to many real systems. The reason for this is that, in any manufacturing system, the influential parameters would be in general different among several stages.

Table 2. Sensitivity study

Case (1)	*Active parameter* (2)		*Optimal α_i* α_1 (3)	α_2 (4)	ATS_{optimal} (5)	$ATS_{\text{convention}}$ (6)	*Ratio R* (7)
1	$g_1 = 1$	$g_2 = 4$	0.001 0835	0.000 4048	463.723	490.265	0.945 86
2	$h_1 = 50$	$h_2 = 300$	0.000 2495	0.003 1364	321.917	454.122	0.708 88
3	$n_1 = 3$	$n_2 = 10$	0.002 4103	0.000 2924	581.421	700.603	0.829 89
4	$\sigma_1 = 0.01$	$\sigma_2 = 0.04$	0.000 0019	0.002 7008	714.924	1006.509	0.710 30
5	$d_1 = 0.01$	$d_2 = 0.05$	0.002 6886	0.000 0141	4074.377	6085.955	0.669 47
6	$p_1 = 0.1$	$p_2 = 0.9$	0.000 4683	0.002 2344	320.297	354.257	0.904 14

The optimal α_i values of the optimal control chart system are also enumerated in Table 2 (columns (3) and (4)). They provide the users with the general guidelines for adjusting the α_i values (or equivalently, the control limit coefficients) for different charts in a system. For example, in case 2, h_i (sampling interval) is the active parameter. In this case, a larger α value should be allocated to the chart with the longer sampling interval. This means that, the control limits of the chart with the longer sampling interval should be made relatively tighter. This scenario is quite heuristic, because, if a chart with a longer sampling interval is capable of giving a signal earlier, the *ATS* value of the system could be reduced to a greater degree. As a guideline, the control limits of the following control charts should be made relatively tighter (or its α_i is set larger):

1. The control chart that is used in a stage with a smaller number of streams.
2. The control chart that has a longer sampling interval.
3. The control chart that has a smaller sample size.
4. The control chart that is used to monitor a process with a larger variance.
5. The control chart that is used to monitor a process with a smaller allowable mean shift.
6. The control chart that is used to monitor a process stage where an out-of-control case is more likely to occur.

With these guidelines in mind, the users can adjust the control limits of each chart in a system rationally and effectively, even if more complicated computation has not been carried out.

Finally, it is interesting to look into the synergistic or anti-synergistic effects between the parameters (e.g., between the sample size n and sampling interval h). Table 3 displays the results of four cases where all the parameters, except n_i and h_i, take their nominal values in both stages. In cases 1 and 2, one, and only one, of the two parameters n and h takes different values in the two stages (in case 1, $n_1 \neq n_2$, but $h_1 = h_2$; in case 2, $h_1 \neq h_2$, but $n_1 = n_2$); the values of the ratio R are significantly smaller than one for both cases. In case 3, $n_1 > n_2$ and $h_1 < h_2$. Both inequalities lead to looser control limits for the optimal control chart in stage 1 and tighter control limits for the optimal control chart in stage 2. The effects of n and h are synergistic, because they enhance each other in each of the two stages. It makes the value of R extremely small (only 0.434 52), or in other words, makes the optimization design very effective. Conversely, in case 4, $n_1 < n_2$ and $h_1 < h_2$. While the first inequality leads to tighter control limits in stage 1 and looser control limits in stage 2, the second inequality results in opposite changes in the control limits in the two stages. In this case, the effects of n and h are anti-synergistic, because they balance out each other in each of the two stages. As a result, the value of R is almost equal to one. In general, the effectiveness of the optimization design is more notable when a synergistic effect exists between the parameters. That is, the differences of all the parameters drive the control limits of some charts in a system to be tighter and the control limits of other charts to be looser.

Table 3. Synergistic or anti-synergistic effects between n and h

Case	n_1	h_1	n_2	h_2	*Ratio R*
1	3	50	10	50	0.802 85
2	3	50	3	300	0.645 87
3	10	50	3	300	0.434 52
4	3	50	10	300	0.994 93

4. Example

A part is machined in a manufacturing system as shown in Fig. 1(a). Stage 1 turns the upper surface (datum: surface 0); stage 2 turns surface 2 (datum: surface 1); stage 3 drills the hole (datum: surface 2); and stage 4 mills the slot (datum: surface 2). The dimensions and tolerances on the drawing are determined by the design engineers. Since the process in stage 4 is much more time consuming, two streams are used in parallel. Among all dimensions, only four (x_1, x_2, x_3 and x_4) obtained at the above four stages are functional (or critical to the overall quality of the part) and have to be closely monitored by the $\bar{X}$ charts. The block diagram of the control chart system is displayed in Fig. 1(b) and the quality linkages in Fig. 1(c). The specifications of the system are listed in Table 4.

Originally, the system adopts the 3σ $\bar{X}$ charts for all the processes, i.e., all charts have the same type-I error

Table 4. The system specifications

Number of stages in the system	$s = 4$
Number of streams	$g_1 = g_2 = g_3 = 1, g_4 = 2$
Sampling intervals (minutes)	$h_1 = h_2 = 100, h_3 = h_4 = 200$
Sample sizes	$n_1 = n_2 = 5, n_3 = n_4 = 6$
In-control process means (mm)	$\mu_{0,1} = 16.00, \mu_{0,2} = 13.00, \mu_{0,3} = 8.00, \mu_{0,4} = 11.00$
Process standard deviations (mm)	$\sigma_1 = 0.020, \sigma_2 = 0.019, \sigma_3 = 0.039, \sigma_4 = 0.018$

probability of 0.0027. As a result, the in-control ATS_0 of the system is equal to 10584 minutes. In order to improve the effectiveness of the control chart system, optimization design is carried out using the algorithms proposed in this article. Thus, some more specifications for d_i, p_i, τ, $\mathbf{V}_i$ and Δ_i are required. The values of the maximum allowable mean shift d_i will be calculated from the upper specification limits USL (shown in Fig. 1(a)) and the minimum allowable process capability ratio $c_{\mathrm{pk,\,min}}$. In this example, $c_{\mathrm{pk,min}}$ is specified as one for all the processes in the manufacturing system. Thus, when PPM hits 2700 in any process, the control chart system is required to provide a signal as soon as possible. The maximum allowable mean shifts are calculated by Equation (4):

$$d_1 = 16.09 - 16.00 - 3 \times 0.020 \times 1 = 0.030 \text{ mm};$$
$$d_2 = 13.07 - 13.00 - 3 \times 0.019 \times 1 = 0.013 \text{ mm};$$
$$d_3 = 8.13 - 8.00 - 3 \times 0.039 \times 1 = 0.013 \text{ mm};$$
$$d_4 = 11.08 - 11.00 - 3 \times 0.018 \times 1 = 0.026 \text{ mm}.$$

For this set of mean shifts, the out-of-control ATS of the conventional 3σ system is equal to 2601 minutes. The probabilities p_i of the out-of-control occurrences are estimated from historical records, which show that the number of out-of-control cases occurring in each of the four stages are four, three, eight and six, respectively. Therefore:

$$p_1 = 4/(4+3+8+6) = 0.190;$$
$$p_2 = 3/(4+3+8+6) = 0.143;$$
$$p_3 = 8/(4+3+8+6) = 0.381;$$
$$p_4 = 6/(4+3+8+6) = 0.286.$$

The QA manager requires that the false alarm rate of the optimal control chart system be maintained at the same level as for the conventional 3σ system. Thus, τ is specified as 10 584 minutes. The dependent relationship vectors $\mathbf{V}_i$ and the formulae for Δ_i were shown in Equations (6) and (7):

$$\mathbf{V}_2 = [1]^T, \quad \mathbf{V}_3 = [2]^T, \quad \mathbf{V}_4 = [2]^T,$$
$$\Delta_2 = \delta_1, \qquad \Delta_3 = \delta_2, \qquad \Delta_4 = \delta_2.$$

So, if stage 1 goes out of control, stage 2 will be directly affected (Equation (A8)):

$$\delta_2 = \Delta_2 = d_1/g_1 = 0.030/1 = 0.030.$$

And stages 3 and 4 will be influenced indirectly (Equation (A7)):

$$\delta_3 = \Delta_3 = \delta_2 = 0.030,$$
$$\delta_4 = \Delta_4 = \delta_2 = 0.030.$$

On the other hand, if stage 2 is out of control, only stages 3 and 4 will be affected:

$$\delta_3 = \Delta_3 = d_2/g_2 = 0.013/1 = 0.013,$$
$$\delta_4 = \Delta_4 = d_2/g_2 = 0.013/1 = 0.013.$$

The computer program *system.c* works out the optimal control chart system for this example in 1.219 CPU seconds on a personal computer (Pentium IV, CPU 1.6 GHz). The results are listed below:

Stage 1: $LCL = 15.965$ mm, $UCL = 16.035$ mm, ($\alpha = 0.000102$);
Stage 2: $LCL = 12.967$ mm, $UCL = 13.033$ mm, ($\alpha = 0.000102$);
Stage 3: $LCL = 7.962$ mm, $UCL = 8.038$ mm, ($\alpha = 0.016590$);
Stage 4: $LCL = 10.976$ mm, $UCL = 11.024$ mm, ($\alpha = 0.000950$);

$$ATS_0 = 10\,584 \text{ minutes } ATS = 1452 \text{ minutes}.$$

It can be observed that, while both the optimal control chart system and the conventional 3σ system have the same ATS_0 value, the out-of-control ATS (=1452) of the optimal system is only 55.8% of that of the conventional system (=2601). This is a significant improvement in effectiveness.

In the optimal solution, the majority of the type-I error probability (or the power) is allocated to stage 3. The reason for this is that this stage has a relatively long sampling interval, a large variance, a small allowable mean shift and a high probability of out-of-control occurrences.

5. Conclusions and discussions

This article discusses the optimization design of a control chart system for use in multi-stage processes. It is found that by properly allocating the power among the individual charts, based on the values of the influential parameters, the effectiveness of the system as a whole can be significantly improved and therefore the product quality is further guaranteed. The improvement in effectiveness is achieved without requiring extra cost and effort for on-line inspection. This is because each chart in the optimal system uses the same sample size and sampling interval as in the conventional system. Most of the specifications of the optimization design are similar to that required by the conventional system design or available from manufacturing information and records. Furthermore, the use of the optimal control chart system will not in any sense increase the difficulties of the shop floor operators to run and understand the control charts. This is because the control charts in the optimal system are almost the same as that in the conventional system, except that the positions of the control limits have been adjusted.

The design algorithm of the optimal control chart system can be easily computerized. The design of a system has to be conducted only once, and the resultant optimal system can be used continuously until the process parameters have changed.

It is believed that the general algorithms discussed in this article can be modified and then applied to the designs of other types of control charts in addition to the $\bar{X}$ chart.

It is also noted that the actual model, layout, scenario and interactions between stages of a particular system may be somewhat different from the model discussed in this article, but the proposed algorithm will be generally applicable. The procedures and formulae can be easily modified to cope with different models.

Finally, the general guidelines for adjusting the control limits of each chart in a system are particularly useful and universally applicable.

References

Ding, Y., Ceglarek, D. and Shi, J. (2002a) Fault diagnosis of multistage manufacturing processes by using state space approach. *ASME Transactions, Journal of Manufacturing Science and Engineering*, **124**, 313–322.

Ding, Y., Ceglarek, D. and Shi, J. (2002b) Design evaluation of multi-station assembly processes by using state space approach. *ASME Transactions, Journal of Mechanical Design*, **124**, 408–418.

Ding, Y., Shi, J. and Ceglarek, D. (2002) Diagnosability analysis of multi-station manufacturing processes. *ASME Transactions*, *Journal of Dynamic Systems, Measurement, and Control*, **124**, 1–13.

Fong, D.D.T. and Lawless, J.F. (1998) The analysis of process variation transmission with multivariate measurements. *Statistica Sinica*, **8**, 151–164.

Hawkins, D.M. (1991) Multivariate quality control based on regression-adjusted variables. *Technometrics*, **33**, 61–75.

Lawless, J.F., MacKay, R.J. and Robinson, J.A. (1999) Analysis of variation transmission in manufacturing processes–part I. *Journal of Quality Technology*, **31**, 131–142.

Montgomery, D.C. (2001) *Introduction to Statistical Quality Control*, Wiley, New York, NY.

Mortell, R.R. and Runger, G.C. (1995) Statistical process control of multiple stream processes. *Journal of Quality Technology*, **27**, 1–12.

Nelson, L.S. (1986) Control chart for multiple stream processes. *Journal of Quality Technology*, **18**, 255–256.

Reynolds, M.R. and Stoumbos, Z.G. (2000) A general approach to modeling CUSUM charts for a proportion. *IIE Transaction*, **32**, 515–535.

Runger, G.C., Alt, F.B. and Montgomery, D.C. (1996) Controlling multiple stream processes with principal components. *International Journal of Production Research*, **34**(11), 2991–2999.

Wade, M.R. and Woodall, W.H. (1993) A review and analysis of cause-selecting control charts. *Journal of Quality Technology*, **25**, 161–169.

Woodall, W. H. and Ncube, M. M. (1985) Multivariate CUSUM quality control procedures. *Technometrics*, **27**(3), 285–292.

Wu, Z., Zhang, X.L. and Yeo, S.H. (2001) Design of the sum-of-conforming-run-length control charts. *European Journal of Operational Research*, **132**(1), 187–196.

Zantek, P.F., Wright, G.P. and Plante, R.D. (2002) Process and product improvement in manufacturing systems with correlated stages. *Management Scinece*, **48**(5), 591–606.

Zhang, G.X. (1989) New diagnosis theory with two kinds of quality, in *ASQC, 43rd Annual Quality Congress Transactions*, pp. 594–599, Toronto, Ontario, Canada.

Appendices

Appendix 1: Calculation of the in-control $\mathbf{ATS_0}$

In a single time unit, the probability that the ith control chart (or a duplicate of the ith chart in a stream) in the ith stage produces a false alarm is approximately equal to α_i/h_i. The probability that it does not produce a false alarm is nearly equal to $(1-\alpha_i/h_i)$. It is recalled that each of the g_i streams in the ith stage runs a duplicate of the ith control chart. Therefore, the probability P_0 that the whole control chart system generates a false alarm in a time unit is:

$$P_0 = 1 - \prod_{i=1}^{s}\left(\prod_{j=1}^{g_i}(1-\alpha_i/h_i)\right) = 1 - \prod_{i=1}^{s}(1-\alpha_i/h_i)^{g_i}. \tag{A1}$$

Finally,

$$ATS_0 = 1/P_0. \tag{A2}$$

Appendix 2: Calculation of the out-of-control ATS

It has been assumed that only one process (i.e., one stream in a stage) in a manufacturing system may go out of control at any moment. The probability w_i that the control charts in the ith stage do not give a signal is calculated differently for the following three cases:

Case 1. Suppose that one of the g_k streams in the kth stage $(1 \le k \le s)$ is out of control (i.e., its mean shift is equal to d_k). The probability β_k of the type-II error that the corresponding control chart fails to give a signal in a single sample is:

$$\beta_k = \Phi\left(\frac{UCL_k - (\mu_{0,k}+\delta_k)}{\sigma_k/\sqrt{n_k}}\right) - \Phi\left(\frac{LCL_k - (\mu_{0,k}+\delta_k)}{\sigma_k/\sqrt{n_k}}\right), \tag{A3}$$

where, the control limits LCL_k and UCL_k are dependent on α_k (Equations (10) and (11)). The probability that none of the g_k duplicates of the kth chart gives a signal in a single sample is:

$$w_k = (1-\alpha_k)^{g_k-1}\beta_k. \tag{A4}$$

Case 2. If the ith stage stays in control and is not influenced by the mean shift in the out-of-control stage k (e.g., in Fig. 1(b), stage 1 is not influenced if mean shift occurs in stage 2, 3 or 4; stage 2 is not impacted if mean shift takes place in stage 3 or 4; and stages 3 and 4 are independent of each other), then, for the duration of one sampling interval h_k of stage k, the probability that a duplicate of the ith chart gives a signal due to type-I error can be approximated by:

$$\theta = \alpha_i h_k / h_i. \tag{A5}$$

The ratio h_k/h_i is used to match the sampling interval h_i in the ith stage to h_k in the kth stage. Thus, the probability that none of the charts in the ith stage gives a signal during a time period of h_k is:

$$w_i = (1-\theta)^{g_i}. \tag{A6}$$

Case 3. If the ith stage stays in control by itself, but its mean value is affected directly or indirectly by the out-of-control stage k, then each of its g_i streams will undergo an induced mean shift:

$$\delta_i = \Delta_i = f_i(\delta_{v_1}, \delta_{v_2}, \ldots), \tag{A7}$$

where, $\delta_{v_1}, \delta_{v_2}, \ldots$ are the output mean shifts of the cause stages (or the immediate upstream stages having impact on the ith stage). The cause stages can be found from the vector $\mathbf{V}_i$ (or the quality linkages). If a cause stage is the out-of-control stage k, the output mean shift is:

$$\delta_k = d_k / g_k. \tag{A8}$$

This is because one, and only one, of the g_k streams in the kth stage is out of control (i.e., having a mean shift of d_k). For the duration of one sampling interval h_k of the out-of-control stage k, the probability that a duplicate of the ith chart gives a signal is calculated by:

$$\theta = (1-\beta_i) h_k / h_i. \tag{A9}$$

This is similar to Equation (A5) except that α_i is replaced by $(1-\beta_i)$, and β_i is calculated by Equation (A3) as β_k. Then, the probability w_i for case 3 can be evaluated by Equation (A6).

Combining all of the three cases, the probability that an out-of-control signal is produced during a time period of h_k can be calculated as:

$$q_k = 1 - \prod_{i=1}^{s} (w_i \mid \text{stage } k \text{ is out of control}). \tag{A10}$$

Therefore, given that one process in the kth stage goes out of control, the value of the out-of-control ATS is:

$$ATS_k = (1/q_k - 1) h_k + 0.5 h_k \tag{A11}$$

This is the steady-state formula, which provides a more realistic evaluation of the out-of-control ATS than the zero-state counterpart (Reynolds and Stoumbos, 2000 Wu *et al.*, 2001). In Equation (A11), $1/q_k$ is actually the average run length, ARL. Since an out-of-control case may occur in any of the s stages, the final ATS for the control chart system is:

$$ATS = \sum_{k=1}^{s} (ats_k \times p_k), \tag{A12}$$

where p_k is the probability that the out-of-control case takes place in the kth stage.

All of the formulae developed in the Appendices have been verified by Monte Carlo simulation. Admittedly, a chart monitoring a process that is currently in control may produce an out-of-control signal (a misleading signal). This is mainly because of the induced mean shifts discussed in case 3. Therefore, whenever a control chart produces an out-of-control signal, all of the upstream processes, which have direct or indirect impacts on this process, must be investigated. More advanced diagnostic methods can be found in many references (Ding, Ceglarek and Shi, 2002a; Ding, Shi and Ceglarek, 2002; Zantek *et al.*, 2002). The type-I error may also generate a misleading signal, but it is negligible.

Biographies

Zhang Wu is an Associate Professor in the School of Mechanical and Production Engineering, Nanyang Technological University, Singapore. His current research interests include the developments of algorithms in quality control, reliability, nonlinear optimization and geometrical tolerance. He is a member of the American Society for Quality.

Ph.D. 1988, McMaster University, Canada.
M.Eng 1984, McMaster University, Canada.
B.Eng 1982, Huazhong University of Science and Technology, China.

Yee Cheong Lam is a Professor in the School of Mechanical and Production Engineering, Nanyang Technological University, Singapore. His current research interests include the development of algorithms for the simulation and optimization of various manufacturing processes. He is a member of the Institution of Engineers, Australia.

Ph.D. 1983, Melbourne University Australia.
B.Eng 1979, Melbourne University Australia.

Sheng Zhang is a Postdoctoral Fellow in the School of Mechanical and Production Engineering, Nanyang Technological University, Singapore. His current research interests include quality control, condition monitoring and fault diagnosis.

Ph.D. 1998, Northeastern University, China.
M.Eng 1996, Northeastern University, China.
B.Eng 1994, Shenyang Institute of Golden Technology, China.

M. Shamsuzaman is a Ph.D. research student in the School of Mechanical and Production Engineering, Nanyang Technological University, Singapore. His current research area is statistical quality control.

M.Eng 2000, Asian Institute of Technology, Thailand
B.Eng 1994, Bangladesh Institute of Technology Chittagong, Bangladesh.

Contributed by the On-line Quality Engineering Department